Available online at www.sciencedirect.com
SCIENCE DIRECT®
Journal of Colloid and Interface Science 263 (2003) 467–472
JOURNAL OF Colloid and Interface Science
www.elsevier.com/locate/jcis

Silica nanobottles templated from functional polymer spheres

Gang Zhang,[a] Yi Yu,[b,c] Xin Chen,[a] Yu Han,[b] Yan Di,[b] Bai Yang,[a,*] Fengshou Xiao,[b] and Jiacong Shen [a]

[a] *Key Laboratory of Supramolecular Structure and Materials, Department of Chemistry, Jilin University, Changchun 130023, People's Republic of China*

[b] *State Key Laboratory of Inorganic Synthesis and Preparative Chemistry, Department of Chemistry, Jilin University, Changchun, China*

[c] *Key Laboratory of Excited Process of Physics, Changchun Institute of Optics, Fine Mechanics and Physics, Chinese Academy of Sciences, Changchun, China*

Received 9 July 2002; accepted 26 March 2003

Abstract

Nanosized hollow silica spheres with holes in the wall (denoted as silica nanobottles) have been successfully prepared by assembly of functional polymer nanospheres with tetraethoxysilane (TEOS) through hydrothermal methods, coupled with removal of the core by programmed calcination. The functional polymer nanospheres were obtained by emulsifier-free emulsion copolymerization of styrene and (ar-vinylbenzyl) trimethylammoium chloride. The silica nanobottle sample was characterized by thermogravimetric analysis (TG), differential thermal analysis (DTA), transmission electron microscopy (TEM), and nitrogen adsorption techniques. The above characterizations confirm that the silica nanobottles have holes of about 8 nm in the wall and this unique structural feature might be useful for their encapsulation. Furthermore, characterization by scanning electron microscopy (SEM), energy dispersive X-ray analysis (EDX), and UV–visible absorption (UV–vis) showed that the luminescent material $Eu(TTA)_3(TPPO)_2$ could be effectively encapsulated in silica nanobottles. This reveals that silica nanobottles have potential applications for nanotechniques.

1. Introduction

Recently, organic/inorganic core–shell particles and micro- or nanosized capsules have received considerable attention for their technological importance in many fields [1–4]. An important extension of core–shell particles is the subsequent removal of the core by either thermal or chemical means [5], forming hollow spheres. Applications of such particles are as capsule agents for drug delivery, catalysis, and protecting sensitive agents such as proteins and enzymes. A variety of procedures currently used to fabricate a wide range of stable hollow spheres of various compositions have been reported. These methods include nozzle reactor systems [6], emulsion/phase separation techniques coupled with sol–gel processing [7], sacrificial core procedures [8,9], and layer-by-layer (LbL) techniques [1,10–14]. There have been some successful examples of the preparation of different kinds of hollow sphere materials (such as silica [1d,2,11], zirconium hydrous oxide [2a], yttrium compounds [2b,3], titania [12,13], copper compounds [14], zeolite [15], and magnetic nanoparticles [2c,4,16]). As particular examples, hollow microspheres with mesoporous walls [17] and with two small holes in the shell [18] have been synthesized from gel composites. Notably, most of these hollow sphere materials have sizes from submicrometer to micrometer, and a few nanosized hollow materials less than 100 nm has been reported [19]. Nanosized hollow spheres are very important as extremely small containers, carriers, and reactors for encapsulation and microreaction in nanotechnology.

On the other hand, facile and flexible strategies that afford fine control over the synthesis and modification of hollow spheres are of great importance in building new classes of colloids. Here we report the preparation of silica nanospheres in a typical precipitation and surface reaction procedure, using a kind of functional polymer nanospheres as templates to synthesize silica nanospheres by hydrothermal methods. The nanosized hollow silica sphere (< 55 nm) with a hole (denoted as a silica nanobottle) was obtained by removal of template functional polymer through programmed calcination at high temperature and the thickness

* Corresponding author.
E-mail addresses: yangbai@jlu.edu.cn (B. Yang), fsxiao@jlu.edu.cn (F. Xiao).

0021-9797/03/$ – see front matter
doi:10.1016/S0021-9797(03)00340-0

of the bottle wall could be easily changed using precursor solutions with different concentrations. Because there is an opening in the hollow cavity of silica nanobottle, it can afford both a channel for transmission and a container for storage. So the silica nanobottle can serve as extremely small containers for encapsulation, as well as nanosized carriers and reactors for catalysis and microreaction. Furthermore, the encapsulation of the rare earth complex $Eu(TTA)_3(TPPO)_2$ in the silica nanobottles reveals a potential application for nanotechniques.

2. Experimental

2.1. Preparation of samples

2.1.1. Functional polymer nanospheres

Cross-linked polymer nanospheres with quarternary ammonium species on the surface were synthesized using emulsifier-free emulsion copolymerization. Styrene was used as the major monomer, and (ar-vinylbenzyl) trimethylammoium chloride (NST, Aldrich) was used as a functional monomer to provide quarternary ammonium species on the surface of nanospheres. The cross-linker was 4,4′-isopropylidene diphenol bimethacrylate (BVA) [20] and the initiator was 2,2′-azobis(2-methylpropionamidine) dihydrochloride (V50, Aldrich), respectively. The weight ratio of styrene:NST:V50:BVA:H_2O for preparing functional nanospheres is at 9.0:0.5:0.02:0.5:100. The polymerization and purifying were carried out according to a published procedure [21], and cross-linked polymer nanospheres with a uniform size of about 45 nm were obtained.

2.1.2. Silica nanobottles

Silica nanospheres were hydrothermally synthesized from the gel mixture of tetraethoxysilane (TEOS, 98 wt%), functional polymer nanospheres (prepared as the above procedure), $NH_3{\cdot}H_2O$ (ammonia, 25 wt%, in water), and H_2O with molar ratio of 1.0:1.1:8.0:20.0. Typically, (1) polymer latex, $NH_3{\cdot}H_2O$, and H_2O were mixed, and then TEOS was added dropwise with vigorous stirring. Finally, the reaction mixture was transferred into a PTFE-lined stainless steel autoclave at 100 °C for 3 days. (2) The solid products were washed with distilled water and dried at ambient temperature. After calcination at 550 °C for 5 h with a heating rate of 2.0 °C/min, the polymer templates were removed and hollow silica spheres were obtained (named silica nanobottles). The preparation process is shown in Scheme 1.

2.1.3. Encapsulation of luminescent RE complex into silica nanobottles

The RE complex $Eu(TTA)_3(TPPO)_2$ (TTA: 1-(2-thenoyl)-3,3,3-trifluoracetate; TPPO: triphenylphosphineoxide) was selected as a guest molecule. Before the encapsulation of the RE complex, the silica nanobottles were modified by APTES (NH_2–$(CH_2)_3Si(OC_2H_5)_3$) [22]. After the modification of

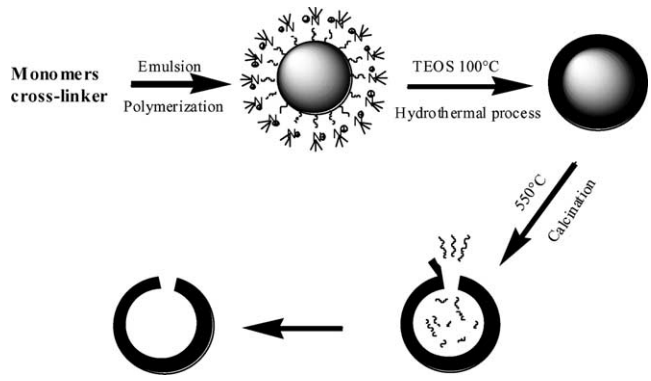

Scheme 1. The procedure for preparation of silica nanobottles.

silica nanobottles, the RE complex was mixed with the silica nanobottles in chloroform (the mass ratio of the modified silica nanobottles to the RE complex is 10:1). The mixtures were stirred at room temperature for 36 h, followed by filtering and washing with chloroform until the filter liquors were no longer luminescent under UV radiation, in order to remove physical adsorption of RE complex on the surface.

2.2. Characterization

Differential thermal analysis (DTA) and thermogravimetric analysis (TG) were performed on a Mettler Netzsch STA 449C themoanalysis instrument. Analyses were carried out under N_2 flow in the range 30–800 °C with a heating rate of 20.0 °C/min. Transmission electron microscopy (TEM) images were conducted on a JEOL 2010 electron microscope with an acceleration voltage of 200 kV. The nitrogen adsorption–desorption isotherms at −196 °C were measured by using a Micromeritics ASAP 2010M system, and the samples were outgassed for 2 h at 400 °C before the measurements. UV–visible absorption spectra of various samples were obtained by a Perkin–Elmer UV-Lambda-20 UV–vis spectrophotometer with $BaSO_4$ as the background in the scanning region of 200–800 nm. Sample size was measured with a S-4200 Scanning Electron Microscope at 20 keV coupled with an energy dispersive X-ray (EDX) analyzer for elemental analysis.

3. Results and discussion

3.1. Thermal analysis

TG/DTA curves of as-prepared sample are shown in Fig. 1. In the DTA curve of the sample (Fig. 1a), there is a broad endothermic peak at about 150 °C, which is related to the desorption of water. In the temperature region 300–550 °C, there is a strong endothermic peak centered at 453 °C, which is due to an endothermic process of depolymerization. Furthermore, in the TG curve of the sample (Fig. 1b), the weight losses in the temperature regions of 25–300, 300–550, and 550–1000 °C are 5, 40, and 2%,

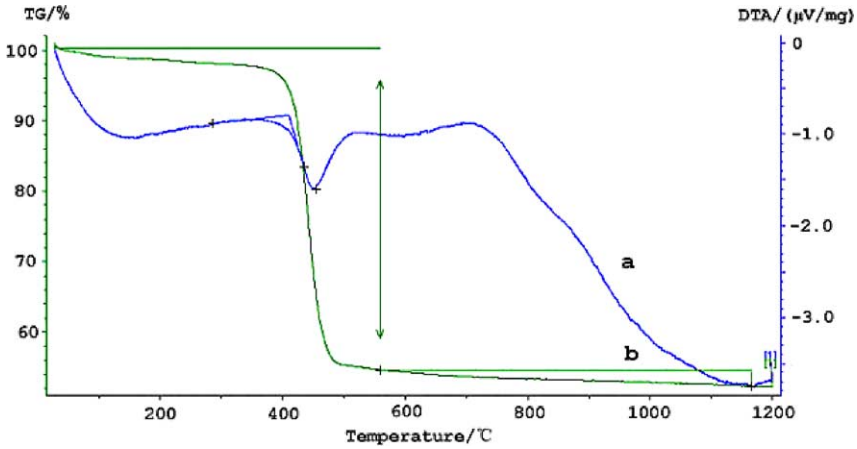

Fig. 1. DTA (a) and TG (b) profiles for the as-prepared sample.

which can be assigned to the removal of adsorbed water, templated polymer, and structural terminal hydroxyl groups in the as-synthesized sample, in good agreement with the DTA results. It is noteworthy that the total weigh loss of the silica sphere sample is about 47%, suggesting that the silica nanobottle has a large pore volume ratio.

3.2. TEM images

Figure 2 shows the TEM images of functional polymer nanospheres from the emulsion polymerization process, as-synthesized silica spheres, and calcined hollow silica samples. Obviously, the functional polymer nanospheres have a uniform particle size, given as 42–45 nm (Fig. 2A). After self-assembly of silica gel with the functional polymer nanospheres, the as-synthesized silica spheres also show a very uniform size at 52–55 nm (Fig. 2B), which are nearly 10 nm thicker than the polymer nanospheres. The difference in diameter between the silica spheres and the polymer nanospheres is reasonably assigned to the thickness of the silica wall, which is well consistent with those reported before [23]. Calcination of the as-synthesized silica spheres at 550 °C for 5 h with an increasing rate of 2.0 °C/min, results in complete removal of the polymer nanospheres, forming hollow spheres with the size of 50–53 nm (Fig. 2C). These data are in close agreement with those obtained from TG analysis. Comparatively, the diameter of calcined silica spheres is about 2 nm smaller than that of the as-synthesized silica spheres, which is explained that silica shell contracted after calcination. Similar phenomena have been observed in the removal of surfactant templates in ordered mesoporous materials [23]. Furthermore, as shown in Fig. 2D, a hole with size 5–8 nm can be seen on the surfaces of some hollow silica spheres. Interestingly, in the insert image of Fig. 2D, it is observed that near the hole, a piece of silica is linked with the silica hollow sphere, and the shape of the piece of silica just fits the hole. These results may suggest that the holes in the silica hollow spheres are formed in the following steps: (1) Calcination at 550 °C leads to decomposition of polymer nanospheres to smaller gas molecules, which have high pressure in the closed hollow spheres. (2) The gaseous molecules with high pressure break through the shells of the hollow spheres, and the hole in the silica hollow sphere is formed. Therefore, these silica hollow spheres with holes are refered as *silica nanobottles*. According to this mechanism, each hollow silica sphere should have one hole. However, as observed in TEM images, only some of the silica hollow spheres can be seen with the hole. This phenomenon can be

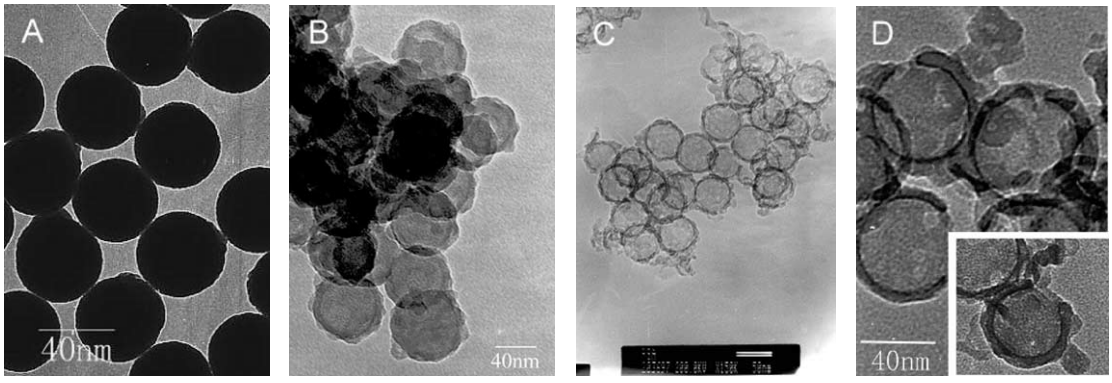

Fig. 2. TEM images of (A) polymer spheres, (B) silica spheres before calcination, (C) hollow silica spheres after calcination, and (D) magnification of silica nanobottles.

interpreted that the holes may appear at any site of the silica hollow spheres and the directions for TEM images are limited for the observation of the hole on the nanobottles.

3.3. Adsorption isotherms

The nitrogen adsorption–desorption isotherms of silica nanobottles and uncalcined silica-coated polymer spheres are well measured. Notably, the adsorption isotherm of silica nanobottles (Fig. 3) exhibits a step rise at high relative pressure (near 0.5). The total BET surface area is at near 278 m^2/g and the total pore volume is estimated at 0.75 cm^3/g, while the uncalcined silica-coated polymer spheres only show very low BET surface areas at 73.4 m^2/g and pore volumes at 0.49 cm^3/g. The comparisons of adsorption results suggest that the calcined sample is a kind of opening hollow sphere (nanobottles). Under ideal conditions, the calcined silica spheres should have a surface area approximately twice as large as that for the uncalcined sample. In our case, however, the surface area value for the uncalcined spheres is somewhat less than expected. There are two possible reasons for this result. (1) From the SEM pictures (Fig. 2B), it can be found that the uncalcined spheres congregated with one another severely, which make a large part of the surface of the spheres inaccessible for N_2 molecules during adsorption measurement and lead to a relatively less surface area value. (2) In the uncalcined sample, there may be some unreacted PS spheres covering the surface of the silica spheres through Si–O–Si connectivity, which can also result in an underestimated value for the surface area. However, in the calcined sample, there is no organic composition and the silica spheres disperse well (Fig. 2C). So the surface area value of the calcined silica spheres should be precise and valuable. The relatively larger pore volume of silica nanobottles may hold a potential for encapsulation of functional compounds in the silica nanobottles.

From the above results, we could propose a mechanism for the formation of nanobottles in the following:

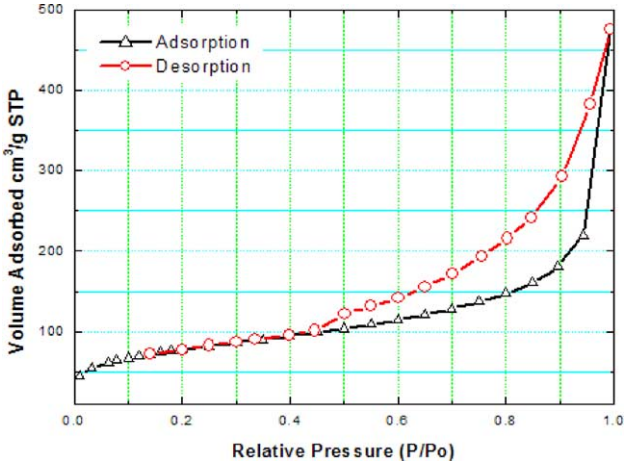

Fig. 3. N_2 adsorption–desorption isotherms for calcined sample (silica nanobottles).

(1) The functional polymer nanospheres with quarternary ammonium cations were copolymerized by styrene and (ar-vinylbenzyl) trimethylammoium chloride in emulsion system. (2) As-synthesized silica-coated polymer nanospheres were hydrothermally prepared from chemical assembly of TEOS with the functional polymer nanospheres. (3) Calcination of as-synthesized silica-coated polymer core–shell spheres at 550 °C results in complete removal of polymer nanospheres, and the hole in the sphere was formed by high pressure resulting from decomposition of polymer nanospheres in the closed hollow silica shell (Scheme 1).

3.4. Encapsulation of RE complex in silica nanobottles

The resulted silica bottles are nanosized materials and there is a hole on the surface of it, which may be useful for the further encapsulations. The RE complex $Eu(TTA)_3(TPPO)_2$ (TTA: 1-(2-thenoyl)-3,3,3-trifluoracetate; TPPO: triphenyl phosphineoxide) was selected as a guest molecule.

Figures 4A and 4B are SEM images of silica nanobottles before and after RE complex encapsulation. The encapsulation sample (Fig. 4B) was washed carefully with chloroform many times. It is obvious that both two images give most like morphology, indicating that the silica nanobottles still remained after the encapsulation of RE complex. Furthermore, the encapsulation of $Eu(TTA)_3(TPPO)_2$ in nanobottles was characterized by energy dispersive X-ray analysis (EDX). In the EDX spectrum of encapsulation sample, the three lines of Eu at 5.80, 6.48, and 6.85 KeV can be easily observed. These results indicate that the RE complex still exists in silica nanobottles after careful washing. To further confirm the encapsulation of the RE complex into silica nanobottles, a UV–visible absorption technique was adopted. Figure 5 shows UV–visible absorption spectra of silica nanobottles, RE complex $Eu(TTA)_3(TPPO)_2$ encapsulated in silica nanobottles, and $Eu(TTA)_3(TPPO)_2$ absorbed on the outer surfaces of as-synthesized silica-coated polymer spheres (after washing with chloroform many times) as well as RE complex $Eu(TTA)_3(TPPO)_2$ itself. The spectrum of silica nanobottles does not show any absorption in the region of 200–800 nm (Fig. 5a); the sample spectrum of

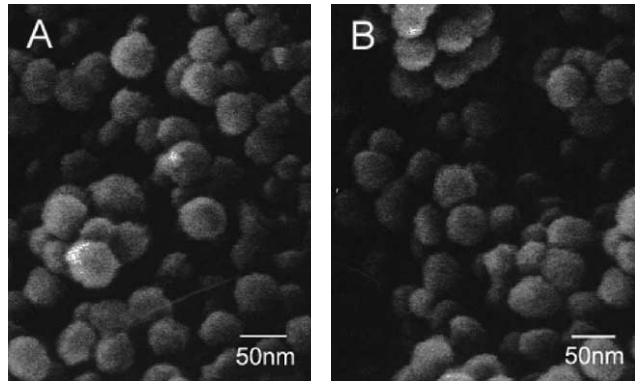

Fig. 4. SEM images of (A) silica nanobottles and (B) silica nanobottles after the encapsulation of RE complex $Eu(TTA)_3(TPPO)_2$.

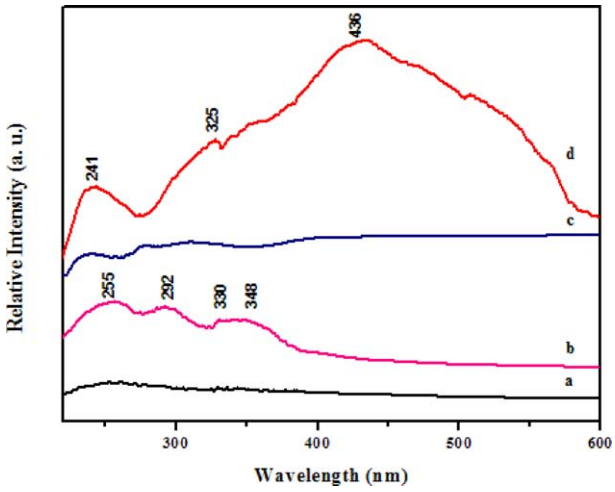

Fig. 5. UV–visible absorption spectra for (a) the modified silica nanobottles, (b) the assembly of $Eu(TTA)_3(TPPO)_2$ in modified silica nanobottles, (c) $Eu(TTA)_3(TPPO)_2$ absorbed on the outer surfaces of as-synthesized silica-coated polymer spheres (after washing with chloroform many times), and (d) the RE complex $Eu(TTA)_3(TPPO)_2$.

RE complex encapsulated in silica nanobottles shows clear peaks near 255, 292, 330, and 348 nm (Fig. 5b); the spectrum of the RE complex absorbed on the outer surfaces of silica nanobottles only shows very weak absorptions after careful washing, which is similar to that of the RE complex (Fig. 5c); the spectrum of $Eu(TTA)_3(TPPO)_2$ shows very strong peaks at 241, 325, and 436 nm (Fig. 5d). From the contrast of the above spectra, it can be confirmed that RE complex absorbed both inner and outer of the hollow spheres. In addition, the peaks at 325 and 436 nm for RE complex are shifted to lower wavelengths 292 and 348 nm for the $Eu(TTA)_3(TPPO)_2$ in silica nanobottles. This phenomenon is possibly assigned to encapsulation of RE complex in silica nanobottles, which is consistent with results for RE complexes entrapped in mesopores of MCM-41 and in microcages of zeolite Y [24].

4. Conclusions

In summary, silica nanobottles have been prepared hydrothermally from preformed functional polymer nanospheres as template. Characterization of TEM and N_2 adsorption results indicate that each nanobottle with particle size of 50–53 nm has a hole of diameter 8 nm. Furthermore, a luminescent RE complex of $Eu(TTA)_3(TPPO)_2$ is successfully encapsulated in silica nanobottles, showing this material has potential application for nanotechnique.

Acknowledgments

This work was supported by the NSFC (29925412, 29825108) and the Major State Basic Research Development Program (G2000078102, G2000077507).

References

[1] (a) F. Caruso, Adv. Mater. 13 (2001) 11;
(b) F. Caruso, Chem. Eur. J. 6 (2000) 413;
(c) F. Caruso, R.A. Caruso, H. Mohwald, Science 282 (1998) 1111;
(d) M. Giersig, T. Ung, L.M. Liz-Marzan, P. Mulvaney, Adv. Mater. 9 (1997) 570;
(e) A.P. Philipse, M.P.B. van Bruggen, C. Pathmamanoharan, Langmuir 10 (1994) 92;
(f) S.Y. Chang, L. Liu, S.A. Asher, J. Am. Chem. Soc. 116 (1994) 6739;
(g) T. Ung, L.M. Liz-Marzan, P. Mulvaney, Langmuir 14 (1998) 3740.
[2] (a) N. Kawahashi, C. Persson, E. Matijevic, J. Mater. Chem. 1 (1991) 577;
(b) N. Kawahashi, E. Matijevic, J. Colloid Interface Sci. 143 (1991) 103;
(c) H. Bamnolker, B. Nitzan, S. Gura, S. Margel, J. Mater. Sci. Lett. 16 (1997) 1412;
(d) D. Walsh, S. Mann, Nature 377 (1995) 320;
(e) A. Garg, E. Matijevic, J. Colloid Interface Sci. 126 (1988) 243;
(f) M.A. Correa-Duarte, M. Giersig, L.M. Liz-Marzan, Chem. Phys. Lett. 286 (1998) 497.
[3] (a) N. Kawahashi, E. Matijevic, J. Colloid Interface Sci. 138 (1990) 534;
(b) H. Gieshe, E. Matijevic, J. Mater. Res. 9 (1994) 436.
[4] (a) H. Shiho, Y. Manabe, N. Kawahashi, J. Mater. Chem. 10 (2000) 333;
(b) H. Shiho, N. Kawahashi, J. Colloid Interface Sci. 226 (2000) 91.
[5] E. Donath, G.B. Sukhorukov, F. Caruso, S.A. Davis, H. Mohwald, Angew. Chem. Int. Ed. Engl. 37 (1998) 2201.
[6] (a) Y. Lu, H. Fan, A. Stump, T.L. Ward, T. Rieker, C.J. Brinker, Nature 398 (1999) 223;
(b) P.J. Bruinsma, A.Y. Kim, J. Liu, S. Baskaran, Chem. Mater. 9 (1997) 2507;
(c) M. Iida, T. Sasaki, M. Watanabe, Chem. Mater. 10 (1998) 3780.
[7] (a) K.J. Pekarek, J.S. Jacob, E. Mathiowitz, Nature 367 (1994) 258;
(b) J.G. Liu, D.L. Wilcox, J. Mater. Res. 10 (1995) 84;
(c) V.V. Hardikar, E. Matijevic, J. Colloid Interface Sci. 221 (2000) 133.
[8] W. Stober, A. Fink, E. Bohn, J. Colloid Interface Sci. 26 (1968) 62.
[9] (a) D.H.W. Hubert, M. Jung, P.M. Frederik, P.H.H. Bowmans, J. Meuldijk, A.L. German, Adv. Mater. 12 (2000) 1286;
(b) F. Caruso, R.A. Caruso, H. Mohwald, Chem. Mater. 11 (1999) 3309;
(c) Y. Yin, Y. Lu, B. Gates, Y. Xia, Chem. Mater. 13 (2001) 1146;
(d) K.H. Rhodes, S.A. Davis, F. Caruso, B. Zhang, S. Mann, Chem. Mater. 12 (2000) 2832.
[10] (a) G. Decher, Science 277 (1997) 1232;
(b) F. Caruso, H. Lichtenfeld, M. Giersig, H. Mohwald, J. Am. Chem. Soc. 120 (1998) 8523;
(c) F. Caruso, Adv. Mater. 11 (1999) 950.
[11] F. Caruso, H. Mohwald, Langmuir 15 (1999) 8276.
[12] (a) Z. Zhong, Y. Yin, B. Gates, Y. Xia, Adv. Mater. 12 (2000) 206;
(b) R.A. Caruso, A. Susha, F. Caruso, Chem. Mater. 13 (2001) 400.
[13] (a) X.C. Guo, P. Dong, Langmuir 15 (1999) 5535;
(b) H. Shiho, N. Kawahashi, J. Colloid Polym. Sci. 278 (2000) 270.
[14] N. Kawahashi, H. Shiho, J. Mater. Chem. 10 (2000) 2294.
[15] X.D. Wang, W.L. Yang, Y. Tang, Y.J. Wang, S.K. Fu, Z. Gao, Chem. Commun. (2000) 2161.
[16] F. Caruso, M. Spasova, A. Susha, M. Giersig, R.A. Caruso, Chem. Mater. 13 (2001) 109.
[17] (a) C.E. Fowler, D. Khushalani, S. Mann, Chem. Commun. (2001) 2028;
(b) C.E. Fowler, D. Khushalani, S. Mann, J. Mater. Chem. 11 (2001) 1968.
[18] H.P. Lin, C.Y. Mou, S.B. Liu, C.Y. Tang, Chem. Commun. (2001) 1970.

[19] (a) K.S. Mayya, D.I. Gittins, A.M. Dibaj, F. Caruso, Nano Lett. 1 (2001) 727;
(b) O.D. Velev, E.W. Kaler, Adv. Mater. 12 (2000) 531;
(c) D.S. Koktysh, X. Liang, B.G. Yun, I. Pastoriza-Santos, R.L. Matts, M. Giersig, C. Serra-Rodriguez, L.M. Liz-Marzan, N.A. Kotov, Adv. Funct. Mater. 12 (2002) 255.
[20] Y. Yang, Y. Li, J. Shen, Chem. J. Chinese Univ. 10 (1989) 276.
[21] X. Chen, Z. Cui, Z. Chen, K. Zhang, G. Lu, G. Zhang, B. Yang, Polymer 43 (2002) 4147.
[22] C.J. Liu, S.G. Li, W.Q. Pang, C.M. Che, Chem. Commun. (1997) 65.
[23] (a) J.S. Beck, J.C. Vartuli, W.J. Roth, M.E. Leonowicz, C.T. Kresge, K.D. Schmitt, C.T.-W. Chu, D.H. Olson, E.W. Sheppard, S.B. McCullen, J.B. Higgins, J.L. Schlenker, J. Am. Chem. Soc. 114 (1992) 10,834;
(b) D.Y. Zhao, J.L. Feng, Q.S. Huo, N. Melosh, G.H. Fredrickson, B.F. Chmelka, G.D. Stucky, Science 279 (1998) 548;
(c) F.S. Xiao, Y. Han, Y. Yu, X.J. Meng, M. Yang, S. Wu, J. Am. Chem. Soc. 124 (2002) 888;
(d) Z.T. Zhang, Y. Han, F.S. Xiao, S.L. Qiu, L. Zhu, R.W. Wang, Y. Yu, Z. Zhang, B.S. Zou, Y.Q. Wang, H.P. Sun, D.Y. Zhao, Y. Wei, J. Am. Chem. Soc. 123 (2001) 5014.
[24] (a) Q.H. Xu, L.S. Li, B. Li, J.H. Yu, R.R. Xu, Micropor. Mesopor. Mater. 38 (2000) 351;
(b) I.L.V. Rose, O.A. Serra, E.J. Nassa, J. Lumin. 72 (1997) 532.